C. R. Mecanique 330 (2002) 527–533

Downstream subsonic jet noise: link with vortical structures intruding into the jet core

Christophe Bogey, Christophe Bailly

LMFA, UMR CNRS 5509, École centrale de Lyon, BP 163, 69134 Écully cedex, France

Received 10 May 2002; accepted 27 May 2002

Note presented by Geneviève Comte-Bellot.

Abstract A subsonic circular jet with a Mach number of 0.9 and a Reynolds number of 65 000 is computed by a compressible Large Eddy Simulation (LES) to determine both the flow field and the sound field in the same calculation. The noise radiated by the jet, provided by LES, is in good agreement with experimental data of the literature in terms of sound pressure spectra, levels and directivity, showing the feasibility of this direct noise calculation. The dominant sound generation mechanism is also investigated, by presenting a correlation between its radiation, observed for an angle of 30° from the downstream direction, and the intrusion of vortical structures into the jet core. ***To cite this article: C. Bogey, C. Bailly, C. R. Mecanique 330 (2002) 527–533.*** © 2002 Académie des sciences/Éditions scientifiques et médicales Elsevier SAS

acoustics / jet noise / computational aeroacoustics / Large Eddy Simulation

Rayonnement acoustique aval des jets subsoniques : lien avec l'intrusion de structures tourbillonnaires dans le cône potentiel

Résumé Un jet circulaire subsonique avec un nombre de Mach de 0,9 et un nombre de Reynolds de 65 000 est calculé par une Simulation des Grandes Echelles (SGE) compressible, afin de déterminer le champ aérodynamique et le champ acoustique dans un même calcul. Le bruit rayonné par le jet, obtenu par SGE, est en bon accord avec les données expérimentales de la littérature, en terme de spectres, de niveaux et de directivité, ce qui démontre la faisabilité de ce calcul acoustique direct. Le mécanisme de production sonore prédominant est également étudié, en présentant une corrélation entre son rayonnement, observé pour un angle de 30° avec la direction de l'écoulement, et l'intrusion de structures tourbillonnaires dans le jet à la fin du cône potentiel. ***Pour citer cet article : C. Bogey, C. Bailly, C. R. Mecanique 330 (2002) 527–533.*** © 2002 Académie des sciences/Éditions scientifiques et médicales Elsevier SAS

acoustique / bruit de jet / aéroacoustique numérique / Simulation des Grandes Echelles

Version française abrégée

Le calcul direct du bruit par résolution des équations de Navier–Stokes compressibles s'est développé grâce à l'utilisation de méthodes numériques propres à l'aéroacoustique [1], et est illustré par ses premières applications tri-dimensionnelles [2–4]. Il permet l'étude des mécanismes de production sonore, puisque le champ acoustique est a priori exact dans le sens où il est obtenu sans aucune modélisation aéroacoustique.

On réalise la Simulation des Grandes Echelles (SGE) d'un jet circulaire à Mach $M = 0{,}9$ et à nombre de Reynolds $Re_D = 65\,000$, afin de montrer la faisabilité de ce calcul et d'étudier les sources de bruit des jets subsoniques. La SGE est particulièrement adaptée à cette étude, car elle calcule les grosses structures

E-mail address: christophe.bogey@ec-lyon.fr (C. Bogey).

S1631-0721(02)01499-7/FLA

turbulentes auxquelles les sources prédominantes sont généralement attribuées. Le code de calcul utilisé est le code ALESIA, construit à l'aide de techniques de l'acoustique numérique [5,6]. Le maillage contient six millions de points, tous les paramètres de la simulation étant décrits dans [7]. Les résultats aérodynamiques tels que l'écoulement moyen, les niveaux et les spectres de la turbulence, les corrélations en deux points, ont été comparés avec succès avec les données de la littérature. Ces comparaisons sont présentées dans [7], et on s'intéresse ici au champ acoustique et aux sources de bruit.

Le champ de dilatation $\Theta = \nabla \cdot \mathbf{u}$ déterminé par SGE est représenté sur la Fig. 1. Les ondes acoustiques produites par le jet apparaissent très nettement, et semblent provenir de la région proche de la fin du cône potentiel du jet, en accord avec les observations expérimentales [8]. Des spectres de pression ont été calculés dans le champ acoustique. On montre ainsi sur la Fig. 2(a) le spectre obtenu pour un angle de 30° par rapport à la direction de l'écoulement. Celui-ci est dominé par les fréquences voisines d'un nombre de Strouhal de $St = 0{,}2$, conformément aux spectres mesurés pour des petits angles d'observation [9,10]. On interprète classiquement ce type de spectre en associant le rayonnement aval des jets aux grandes structures de l'écoulement. Les niveaux sonores ont alors été calculés et représentés sur la Fig. 2(b). Ils sont en très bon accord avec les niveaux mesurés sur des jets au même nombre de Mach et avec des nombres de Reynolds variés [9,11,12]. La dispersion des niveaux pour des angles supérieurs à 60° est attribuée à un effet du nombre de Reynolds, car la contribution des sources de bruit liées à la turbulence fine n'est plus négligeable dans cette zone.

On étudie maintenant la source de bruit prépondérante en aval, localisée au niveau de la fin du cône potentiel, associée aux grosses structures, mais non encore bien identifiée [13]. La pression et la norme du vecteur vorticité $|\omega|$ ont été enregistrées pendant un temps de $t^* = tU_j/D = 39{,}6$. Le signal de pression au point ($x = 24{,}8r_0$, $y = 8r_0$, $z = 0$), pour un angle de 30° par rapport à la direction de l'écoulement, est alors tracé sur la Fig. 3. Il présente une oscillation avec une période correspondant en moyenne au nombre de Strouhal de $St \simeq 0{,}2$ observé dans le spectre de la Fig. 2(a). Le front d'onde de plus grande amplitude est obtenu à $t^* = 13{,}2$. En évaluant le temps de propagation acoustique, le temps d'émission de cette onde doit être légèrement supérieur à $t^* \simeq 6{,}1$. Le champ de vorticité dans le plan $z = 0$ est ainsi représenté sur la Fig. 4, à $t^* = 6{,}2$ et à $t^* = 7{,}5$. Cette figure suggère que les structures turbulentes des couches cisaillées font irruption dans le cône potentiel du jet, et sont brusquement accélérées.

On construit un indicateur de la présence de structures tourbillonnaires dans le jet, avec $\delta_{sl}(x)$ la distance entre les zones cisaillées déterminée à l'aide d'un seuil de vorticité $|\omega|$ de 5×10^4 s^{-1}. Une représentation spatio-temporelle de δ_{sl} est donnée sur la Fig. 5. Les zones en noir, définies pour $\delta_{sl} \leqslant 0{,}05r_0$, sont distribuées régulièrement dans le temps, et montrent que les couches cisaillées pénètrent dans le jet de manière intermittente et quasi-périodique à la fin du cône potentiel, et sont alors entraînées par la vitesse longitudinale.

L'évolution temporelle de δ_{sl} pour $x = 12{,}1r_0$ est tracée sur la Fig. 6. Les entrées des structures tourbillonnaires des couches cisaillées dans le cône potentiel corespondent aux annulations de δ_{sl}. Pour relier ces événements au champ acoustique, le signal de pression de la Fig. 3 est aussi représenté sur la Fig. 6, un décalage temporel étant appliqué entre les deux signaux pour prendre en compte le temps de propagation. On constate que les pics négatifs de pression coïncident avec les annulations de δ_{sl}. Cette bonne corrélation montre que le bruit basse fréquence prédominant en aval du jet est relié à l'intrusion des couches cisaillées de vitesse dans le jet.

1. Introduction

Methods for computing both the flow field and the acoustic radiation directly from the resolution of the unsteady compressible Navier–Stokes equations have been developed in the last decade. The advantages of this approach are first to provide an a priori exact sound field because no acoustic model is used, and second

to permit the investigation of the acoustic sources from instantaneous flow and acoustic quantities. However, to compute sound waves with sufficient accuracy, it is necessary to use techniques of Computational AeroAcoustics (CAA) which account for the great difference of levels and length scales between flow and acoustic quantities [1]. CAA has been applied to the three methods commonly used to solve the Navier–Stokes equations: Direct Numerical Simulation (DNS) where all turbulent scales are computed, Large Eddy Simulation (LES) where only large scales are calculated, and the unsteady Reynolds Averaged Navier–Stokes equations (URANS). Among the first 3-D applications are the DNS of a subsonic circular jet by Freund [2], the LES of a supersonic rectangular jet by Morris et al. [3], and the study of screech tones in round jets using URANS by Shen and Tam [4].

In the present study, the LES of a circular jet with a Mach number $M = 0.9$ and a Reynolds number $Re_D = U_j D/\nu = 65\,000$ is performed. The motivation is to show the feasibility of the direct computation by LES of the sound generated by a subsonic jet, and then to investigate sound generation mechanisms. The use of LES is important because it can be applied to flows with Reynolds numbers higher than is possible with DNS. LES is also appropriate for studying jet noise where it is well recognized that large-scale structures play a predominant role, even though the generation mechanisms are not clearly identified for subsonic jets.

The simulation code used in this work is a 3-D extension of the ALESIA code [5], developed especially for acoustic simulations with CAA numerical methods, including the non-dispersive DRP scheme [1] and a far-field formulation of the boundary conditions [6]. All parameters of the simulation can be found in [7]. The computational grid encompasses the entire jet, and the acoustic field is only calculated in a slice above the jet. This allows the size of the grid to be kept to six million points. The dimensionless simulation time is $TU_j/D = 300$, which is long enough to achieve statistical convergence both for the flow and for the sound field. Flow characteristics, namely meanflow parameters, turbulence intensities and spectra, integral length scales, and two-point correlations, have been successfully compared with corresponding measurements [7]. In what follows, we focus on the acoustic results given by the LES. The computed sound field is described in Section 2. Then the dominant sound source is investigated in Section 3.

2. Acoustic field provided by LES

Fig. 1 displays, in the plane $z = 0$, the vorticity field ω_z in the flow and the dilatation field $\Theta = \nabla \cdot \mathbf{u}$ outside, both being obtained directly from the simulation. Acoustic wave fronts generated by the jet are clearly visible, and they originate mainly from the region where the mixing layers merge, around $x = 11r_0$. Dominant sound sources are apparently found in the region near the end of the jet potential core, in accordance with experimental observations [8].

To characterize the sound field, pressure spectra have been calculated in the acoustic field. For example, Fig. 2(a) shows the spectrum obtained for an angle of 30° from the outlet axis, for a distance of $60r_0$ from the jet nozzle to make later comparisons with experimental directivities. It is dominated by low frequency components, with a peak around a Strouhal number $St = 0.2$. This spectrum has been observed experimentally for low observation angles, as illustrated by measurements of Stromberg et al. [9] on a $M = 0.9$, $Re_D = 3.6 \times 10^3$ jet, and those of Long and Arndt [10] on a $M = 0.52$, $Re_D = 8.5 \times 10^4$ jet. The classical interpretation is that for low angles, jet noise is mainly associated to the large-scale turbulent structures, and is insensitive to variations in the Reynolds number.

The sound pressure levels, calculated by integrating the sound spectra, are presented in Fig. 2(b). They are in very good agreement for all observation angles with experimental data from jets with similar Mach numbers but various Reynolds numbers [9,11,12]. As expected, the acoustic levels reach a peak for an angle about $\theta = 30°$. For higher angles, the levels of the computed $Re_D = 6.5 \times 10^4$ jet stand between the levels measured for the $Re_D = 3.6 \times 10^3$ jet, and for the $Re_D \simeq 5 \times 10^5$ jets. This can be attributed to a Reynolds number effect, since the fine-scale turbulence, which becomes important at high Reynolds numbers, generates sound which must be taken into account at wide observation angles.

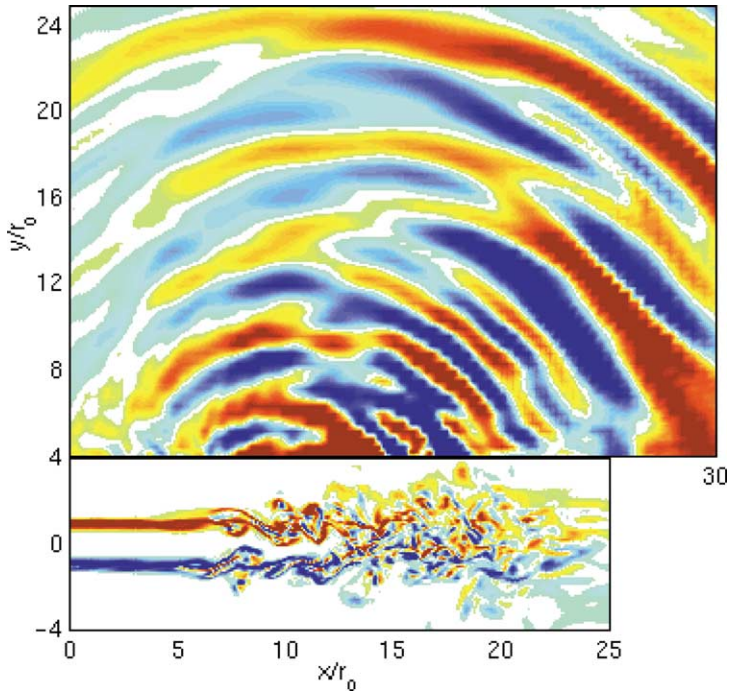

Figure 1. Snapshots, in the x–y plane at $z = 0$, of the vorticity ω_z in the flow and of the dilatation $\Theta = \nabla \cdot \mathbf{u}$ outside. The vorticity color scale is from -3.8×10^5 to 3.8×10^5 s^{-1}, the dilatation scale from -90 to 90 s^{-1}.

Figure 1. *Vues instantanées, dans le plan $z = 0$, de la vorticité ω_z dans l'écoulement et de la dilatation $\Theta = \nabla \cdot \mathbf{u}$ en dehors. Les échelles de couleur sont définies pour des niveaux de vorticité allant de $-3{,}8 \times 10^5$ à $3{,}8 \times 10^5$ s^{-1}, et pour des niveaux de dilatation de -90 à 90 s^{-1}.*

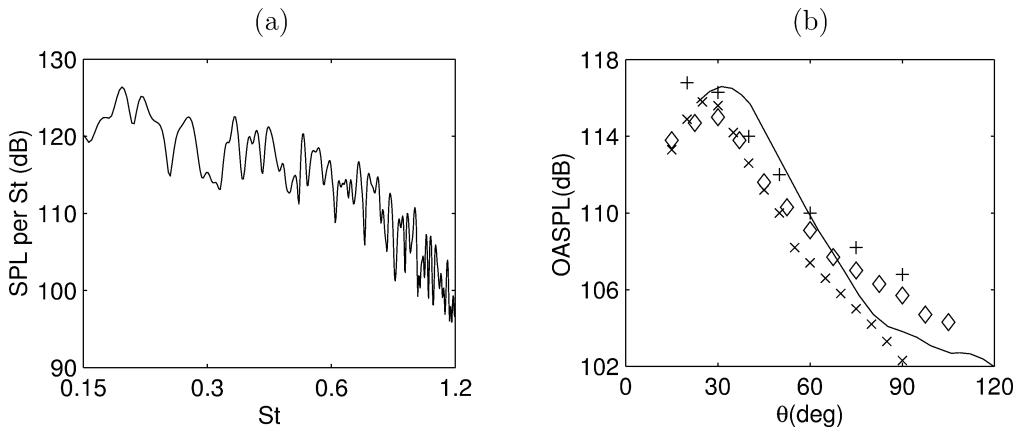

Figure 2. (a) Acoustic pressure spectrum at $60r_0$ from the inflow, for an angle of 30° from the jet axis, as a function of $St = fD/U_j$. (b) Overall sound pressure levels at $60r_0$ from the jet nozzle, as a function of observation angle θ. Experimental data by: ×, Stromberg et al. [9] ($M = 0.9$, $Re_D = 3600$); +, Mollo-Christensen et al. [11] ($M = 0.9$, $Re_D = 5.4 \times 10^5$); ⋄, Lush [12] ($M = 0.88$, $Re_D = 5 \times 10^5$).

Figure 2. (a) *Densité spectrale de puissance de la pression acoustique à une distance de $60r_0$ de la sortie de buse, pour un angle de 30° par rapport à l'axe du jet, en fonction de $St = fD/U_j$.* (b) *Niveaux sonores à une distance de $60r_0$ de la sortie de buse, en fonction de l'angle d'observation θ.*

The similarity between the acoustic results obtained for jets with very different Reynolds numbers suggests that the dominant sound source in the downstream direction is independent of the Reynolds number. Considering the good agreement of numerical results with experiments, this source is likely to be well described in the simulation, and we can now investigate it by tracking a link between the acoustic emission and the dynamics of the large turbulent structures.

3. Investigation of the dominant sound source

The dominant sound source in subsonic jets, associated to larges structures, has not been clearly identified, although its location near the end of the potential core has been well established [8]. Hussain [13], for instance, has suggested that it is the breakdown process of the toroidal structures into substructures near the end of the jet core. In the present work, movies from both the flow and the acoustic radiation show that the noise generated in the downstream direction appears to be attributable to the merger of opposite sides of the shear annulus at the end of the potential core. To demonstrate this, the radiated acoustic pressure and the norm of the vorticity vector $|\omega|$ in the jet have been recorded during the time $t^* = tU_j/D = 39.6$.

To study the dominant noise mechanism, the time evolution of pressure is plotted for the point ($x = 24.8r_0,\ y = 8r_0,\ z = 0$) in Fig. 3. This point is located at a distance of $16r_0$ from the apparent source location, ($x = 11r_0,\ y = z = 0$), with an angle of 30° with respect to the downstream direction. The pressure signal has a low frequency periodic behaviour with a period corresponding to the Strouhal number of $St \simeq 0.2$ emerging in the spectrum of Fig. 2(a).

To detect the sound source, the wave front with the highest amplitude is considered, and it is found for $t^* = 13.2$. A time delay of $\Delta t_r^* = \Delta t_r U_j/D = 7.1$ between the emission of this wave and its arrival at the observation point is calculated if the propagation from the source location ($x = 11r_0,\ y = z = 0$) to the observer occurs at the mean acoustic velocity. We will see that the appropriate Δt_r^* is smaller because a significant amount of the propagation takes place within the $M = 0.9$ flowfield. The vorticity field is therefore shown at times $t^* = 6.2$ and $t^* = 7.5$ in Fig. 4 in the plane $z = 0$. The shear layers can be differentiated up to $x = 15r_0$ in Fig. 4(a), but only up to $x = 11r_0$ in Fig. 4(b). Turbulent structures originating from the shear layers have penetrated into the jet core near $x = 10r_0$, and they have been suddenly accelerated by the higher flow velocity.

To look for a correlation between the intrusion of vortical structures into the jet core and the sound radiation in the downstream direction, an indicator of the presence of vortical structures in the vicinity of the jet axis is introduced. The transverse distance $\delta_{sl}(x)$ between the shear layers in the plane $z = 0$ is computed using the threshold of magnitude vorticity $|\omega| \leqslant 5 \times 10^4\ \mathrm{s}^{-1}$. A space-time representation of δ_{sl} is provided in Fig. 5 for $10r_0 \leqslant x \leqslant 14r_0$. The black-colored regions, determined from the criterion $\delta_{sl} \leqslant 0.05r_0$, indicate that vortical structures are significantly found in the jet core. Horizontal lines, accounting for the

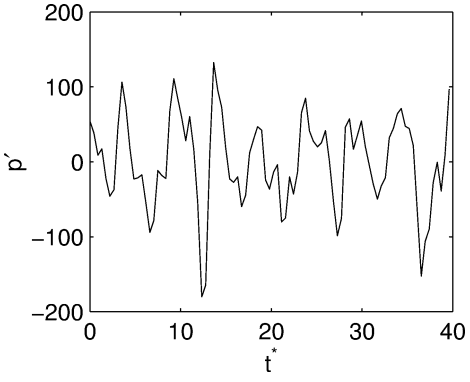

Figure 3. Time evolution of the acoustic pressure in Pa at the point ($x = 24.8r_0,\ y = 8r_0,\ z = 0$), as a function of $t^* = tU_j/D = 1/St$.

Figure 3. *Evolution temporelle de la pression acoustique en Pa au point* ($x = 24{,}8r_0,\ y = 8r_0,\ z = 0$), *en fonction de* $t^* = tU_j/D = 1/St$.

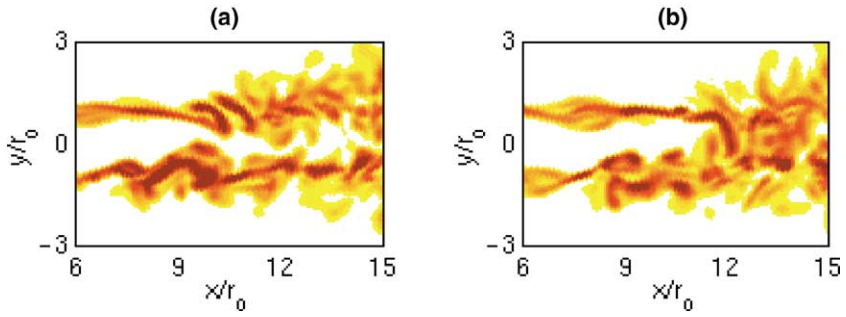

Figure 4. Snapshot of the vorticity norm $|\omega|$ in the plane $z = 0$: (a) at $t^* = 6.2$; (b) at $t^* = 7.5$. The color scale is from 6×10^4 to 30×10^4 s^{-1}.

Figure 4. *Vue instantanée de la norme de la vorticité* $|\omega|$ *dans le plan* $z = 0$: (a) *à* $t^* = 6{,}2$; (b) *à* $t^* = 7{,}5$. *L'échelle de couleur est définie pour des niveaux allant de* 6×10^4 *à* 30×10^4 s^{-1}.

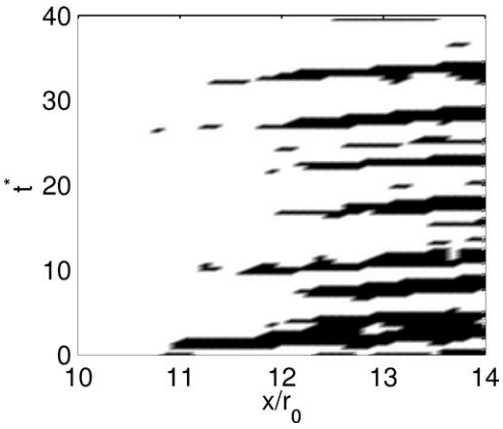

Figure 5. Space–time evolution of the distance between the shear layers δ_{sl} in the plane $z = 0$. The regions in black are for $\delta_{sl} \leqslant 0.05 r_0$.

Figure 5. *Evolution spatio–temporelle de la distance entre les zones cisaillées dans le plan* $z = 0$. *Les zones en noir sont caractérisées par* $\delta_{sl} \leqslant 0{,}05 r_0$.

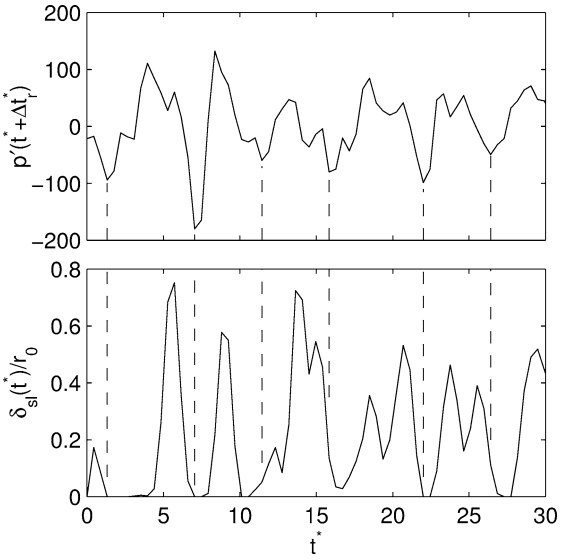

Figure 6. Time traces of the acoustic pressure $p'(t^* + \Delta t_r^*)$ at the point $(x = 24.8 r_0,\ y = 8 r_0,\ z = 0)$, and of the distance between the shear layers $\delta_{sl}(t^*)$ for $x = 12.1 r_0$, with $\Delta t_r^* = 5.3$.

Figure 6. *Traces temporelles de la pression acoustique* $p'(t^* + \Delta t_r^*)$ *au point* $(x = 24{,}8 r_0,\ y = 8 r_0,\ z = 0)$, *et de la distance entre les zones cisaillées* $\delta_{sl}(t^*)$ *à* $x = 12{,}1 r_0$, *avec* $\Delta t_r^* = 5{,}3$.

convection of these structures by the longitudinal velocity, are observed. Starting around $x = 12 r_0$, they are well distinct and regularly distributed in time. This shows that turbulent structures of the shear layers come into the jet quasi-periodically, in the vicinity of $x = 11 r_0$.

The time evolution of δ_{sl} for $x = 12.1 r_0$ is plotted in Fig. 6. Periods when δ_{sl} is small correspond to the intrusion of vortical structures across the center-line of the jet. The period of cancellations of δ_{sl} is about 5 in dimensionless time, which corresponds to a Strouhal number of 0.2. We note that this is close to the peak

observed in Fig. 2(a). To link these intrusions with the acoustic field, the pressure signal of Fig. 3 is also plotted in Fig. 6, in order to determine if the two signals are correlated. A time delay $\Delta t_r^* = 5.3$ is applied between the two signals to account for the propagation time. This value has been determined to match the minimum in the pressure signal with the associated cancellation of δ_{sl}. The same periodicity is observed on both signals, and the negative pressure peaks clearly correspond to the cancellations of the distance between the shear layers. This correlation demonstrates that the dominant low frequency noise radiated in the downstream direction is connected to the intermittent intrusion, into the jet core, of vortical structures originating from the shear layers.

4. Conclusion

The present simulation of a subsonic circular jet with a Mach number of 0.9 and a Reynolds number of 6.5×10^4 shows the feasibility of the direct computation of the sound using LES, and gives support to the fact that numerical simulations now provide new opportunities to study and assess noise generation mechanisms. In particular, the dominant acoustic radiation in the downstream direction, which occurs for any Reynolds number, has been investigated. It has been shown that the intrusion into the jet core of vortical structures originating from the shear layers could be responsible for this radiation. The noise generation mechanism appears to be associated to the periodic sudden accelerations of these structures when entering into the high speed jet core. For noise production at wider angles, other sound sources have to be taken into account in addition to the one described in this work.

Acknowledgements. This work was supported by the RRIT « Recherche Aéronautique sur le Supersonique » (Ministère de la Recherche). Computing time was supplied by the Institut du Développement et des Ressources en Informatique (IDRIS-CNRS).

References

[1] C.K.W. Tam, Computational aeroacoustics: issues and methods, AIAA J. 33 (10) (1995) 1788–1796.
[2] J.B. Freund, Noise sources in a low-Reynolds-number turbulent jet at Mach 0.9, J. Fluid Mech. 438 (2001) 277–305.
[3] P.J. Morris, L.N. Long, T.E. Scheidegger, Parallel computations of high speed jet noise, AIAA Paper 99-1873.
[4] H. Shen, C.K.W. Tam, Numerical simulation of the generation of the axisymmetric mode jet screech tones, AIAA J. 36 (10) (1998) 1801–1807.
[5] C. Bogey, C. Bailly, D. Juvé, Numerical simulation of the sound generated by vortex pairing in a mixing layer, AIAA J. 38 (12) (2000) 2210–2218.
[6] C. Bogey, C. Bailly, Three-dimensional non-reflective boundary conditions for acoustic simulations: far field formulation and validation test cases, Acustica (2002), to appear.
[7] C. Bogey, C. Bailly, D. Juvé, Noise investigation of a high subsonic, moderate Reynolds number jet using a compressible LES, Theoret. Comput. Fluid Dynamics (2002), submitted. See also AIAA Paper 2000-2009.
[8] D. Juvé, M. Sunyach, G. Comte-Bellot, Intermittency of the noise emission in subsonic cold jets, J. Sound Vibration 71 (3) (1980) 319–332.
[9] J.L. Stromberg, D.K. McLaughlin, T.R. Troutt, Flow field and acoustic properties of a Mach number 0.9 jet at a low Reynolds number, J. Sound Vibration 72 (2) (1980) 159–176.
[10] D.F. Long, R.E.A. Arndt, Jet noise at low Reynolds number, AIAA J. 22 (2) (1984) 187–193.
[11] E. Mollo-Christensen, M.A. Kolpin, J.R. Martucelli, Experiments on jet flows and jet noise far-field spectra and directivity patterns, J. Fluid Mech. 18 (1964) 285–301.
[12] P.A. Lush, Measurements of subsonic jet noise and comparison with theory, J. Fluid Mech. 46 (3) (1971) 477–500.
[13] A.K.M.F. Hussain, Coherent structures and turbulence, J. Fluid Mech. 173 (1986) 303–356.